# Ground-based Measurement of Millimetre-wavelength Emission by Upper Stratospheric $O_2$

J. W. WATERS

Research Laboratory of Electronics and Department of Electrical Engineering, Massachusetts Institute of Technology, Cambridge, Massachusetts 02139

**Measurements from ground level of 53 GHz radiation from molecular oxygen in the stratosphere, using a very precise radiometer, can be used to give stratospheric temperatures.**

THIS article reports measurements at sea level of upper stratospheric thermal emission from five high-rotational, millimetre-wavelength, magnetic dipole transitions of molecular oxygen, and discusses use of the emission lines for remote sensing of upper stratospheric temperatures. One of the lines, the $27_-$, has been reported earlier in solar absorption[1] and in emission[2] but with poorer signal-to-noise and frequency-resolution than the measurements given here, and wings of some of the lines are evident in previous aircraft absorption measurements[3]. Stratospheric emission lines of submillimetre wavelength have also been observed recently from aircraft by a different technique[4,5].

Molecular oxygen has a band of spectral lines near 60 GHz (5 mm wavelength) and a single line at 118 GHz produced by changes in orientation of its electronic spin relative to its rotation. The individual spin-rotation lines are designated $N_+$ or $N_-$, where $N$ is the rotation quantum number which must be odd for $^{16}O_2$ in the $^3\Sigma_g^-$ electronic ground state, and where the subscript indicates whether the change in total angular momentum of the molecule during an emission transition is $+1$ or $-1$. Each $N_\pm$ line has $3(2N\pm1)$ Zeeman components spread over $\sim\pm1$ MHz by the terrestrial magnetic field. Near the centre of the 60 GHz band the terrestrial atmosphere is quite opaque, but on the band edges thermal emission, originating in the upper stratosphere where the lines are relatively narrow, can penetrate the lower atmosphere and can be measured at the ground.

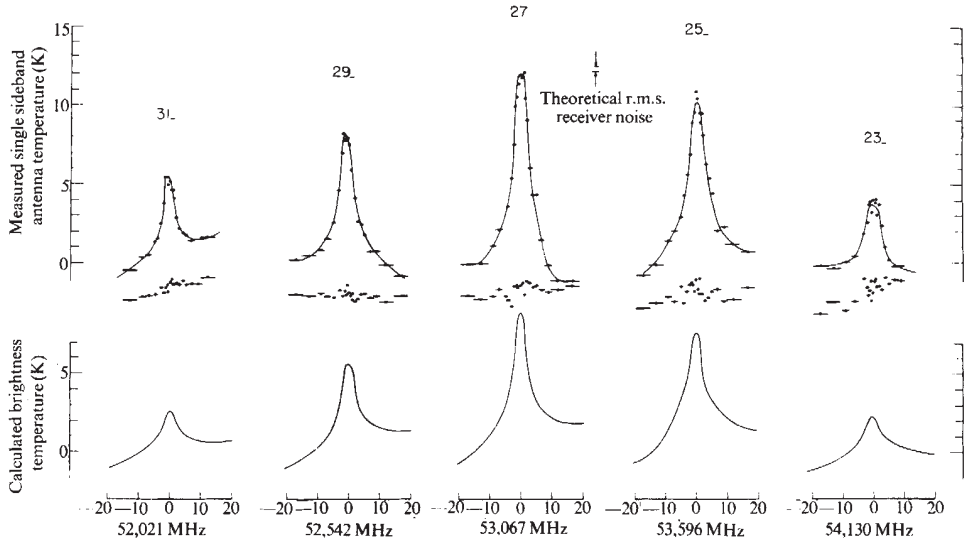


**Fig. 1** Measured (upper) and calculated (lower) atmospheric zenith emission. Each measured line and the instrumental baseline shown beneath it represent integration for 16 min. The measurements were made during the week of August 30, 1972.

The measurements reported here were made during very clear sky conditions at Haystack Observatory (elevation 0.15 km) in Westford, Massachusetts, with a radiometer constructed at the Massachusetts Institute of Technology[6]. The radiometer was a load-switched superheterodyne microwave receiver with a noise temperature of 1,800 K and no rejection of the image sideband. A linearly polarized standard-

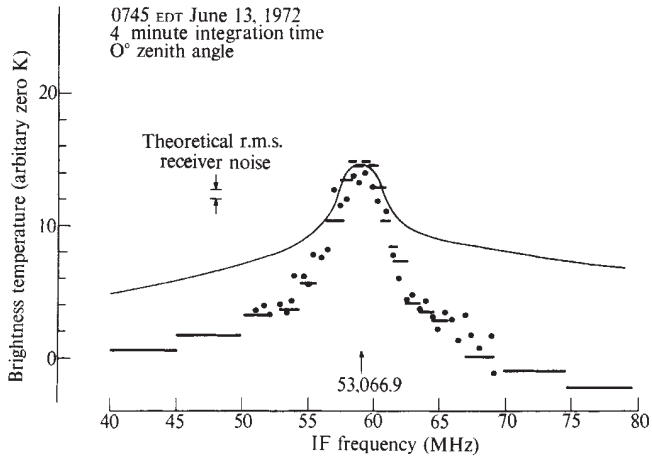


**Fig. 2** Measured and calculated zenith emission from the 27_ line. The zero levels of the measured and calculated lines are adjusted to give agreement at line centre. ▬, Filter system measurements; ●, haystack correlator measurements; ——, calculated for 1962 US standard atmosphere.

gain microwave horn (10° beamwidth) was the antenna. The local oscillator, a klystron phase locked to a crystal reference, had frequency stability and absolute accuracy of $10^{-2}$ MHz. Spectral analysis was performed both by a twenty-three-channel filter bank and by the 100-channel Haystack digital autocorrelator[7]. The filter bank covered a total bandwidth of 40 MHz, with individual filters having resolutions ranging from 0.5 MHz for the centre channels to 5.0 MHz for the outer channels. Two bandwidths were used with the autocorrelator: 20 MHz with 0.5 MHz resolution, and 6.67 MHz with 0.16 MHz resolution. A small digital computer processed data from the filter bank. Data from the autocorrelator were Fourier-transformed and further processed by the Haystack computer.

**Table 1** Centre Frequencies, $\nu_0$, and Base (−20 MHz from the Line Centre) Absolute Zenith Brightness Temperatures, $T_B$, for the Oxygen Lines

| Transition | Measured $\nu_0$ (MHz) | Calculated (−20 MHz from line centre) $\tau$ (nepers) | $T_B$ (K) | $T_B$, including image sideband (K) | Measured $T_B$, including image sideband (K) |
|---|---|---|---|---|---|
| 23_ | 54,130.2±0.5 | 3.30 | 269 | 267 | 265± 2 (U) |
| 25_ | 53,595.9±0.2 | 2.03 | 241 | 242 | 240± 5 (L) |
| 27_ | 53,066.9±0.2 | 1.27 | 198 | 194 | 206±10 (U) |
| 29_ | 52,542.4±0.2 | 0.88 | 161 | 163 | 174±12 (L) |
| 31_ | 52,021.4±0.5 | 0.64 | 129 | 131 | 139±15 (L) |

Uncertainties in the frequencies are attributable to the uncertainties in fitting the measured emission to the calculated emission; frequencies for the 25_, 27_ and 29_ lines are more accurate because they were observed with 0.16 MHz autocorrelation resolution. Uncertainties in measured absolute temperatures are attributable to the 10% calibration uncertainty. Beside the measured base temperature is indicated whether the line was observed in the upper (U) or lower (L) sideband. The zenith opacity $\tau$ calculated for the base of the lines is also given.

Figs. 1–3 show, with an increasingly expanded frequency scale, the measurements and the results of calculations. The intensities of the lines increase with frequency up to the 27_ line because the lower rotational states have larger populations, but decrease with frequency above the 27_ because of increasing attenuation by the lower atmosphere. A similar set of $N_+$ lines exists on the high-frequency band edge. The linewidths of the measured emission correspond to pressures less than 10 mbar, proving that the emission originated at altitudes above 30 km. Table 1 gives the measured line frequencies, which agree to within measurement accuracy with the calculated values[8] (see also refs. 9 and 10). For each line, the local oscillator frequency was shifted slightly in a separate measurement to make certain in which sideband the line appeared. The vertical axis of each figure is the brightness (equivalent blackbody radiation) temperature of the emission. Absolute accuracy of the measured amplitudes is 10% as determined by calibration of the radiometer with liquid nitrogen and thermal loads, and zero levels in the figures are arbitrary; Table 1 gives absolute values for measurements and calculations. Instrumental baselines, measured at each observed line frequency by tipping the radiometer so the horn antenna was pointed at or below the horizon, where no spectral feature is expected, are shown beneath the measured lines in Fig. 1. Fig. 2 indicates the excellent agreement between spectral analysis by the filter bank and the autocorrelator. The high-frequency resolution measurement shown in Fig. 3 represents equal observation times with the observed electric vector respectively parallel and perpendicular to the Earth's magnetic field. As expected for the latitude of the measurement, no polarization was observed.

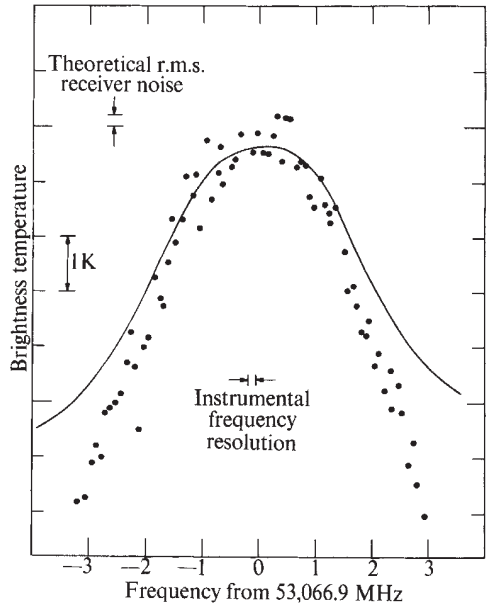


**Fig. 3** High-resolution measurement and calculation of zenith emission from the 27_ line. The measurement was made 0200–0600 EST, August 30, 1972. ●, Measured; ——, calculated.

Calculations of millimetre wavelength absorption by $O_2$, first performed by Van Vleck[11], have been presented by several workers (refs. 12–17 and unpublished work of H. J. Liebe and W. M. Welch for the AGARD electromagnetic wave propagation panel). Zeeman splitting of the spin-rotation lines must be accounted for above ~45 km in the terrestrial atmosphere, where collisional broadening is sufficiently small that it does not mask the splitting. Lenoir[12] developed expressions to describe the polarized and anisotropic emission from the Zeeman components in the presence of a magnetic field and calculated emission from the mesosphere as seen from above. The calculations done here use Lenoir's matrix radiative transfer equations with the 1962 US Standard Atmosphere model[18], a magnetic latitude of 55° (at which the measurements were made), and a vector dipole model of the Earth's magnetic field[18]. Techniques used in the calculations

are described elsewhere[19]. A volume mixing ratio of 0.21 is assumed for $O_2$ and integrations are carried to 90 km. The Gross[20], or Zhevakin-Naumov[14], line shape is used with linewidth equal to the geometrical sum of Doppler[12] and collision[17] widths. "Zero frequency", $\Delta J=0$, $O_2$ transitions[11] are included by adding their absorption to the diagonal elements of the absorption coefficient matrix. Absorption by atmospheric water vapour and other minor constituents is thought negligible ($\sim 0.05$ neper) and is not included in the calculations.

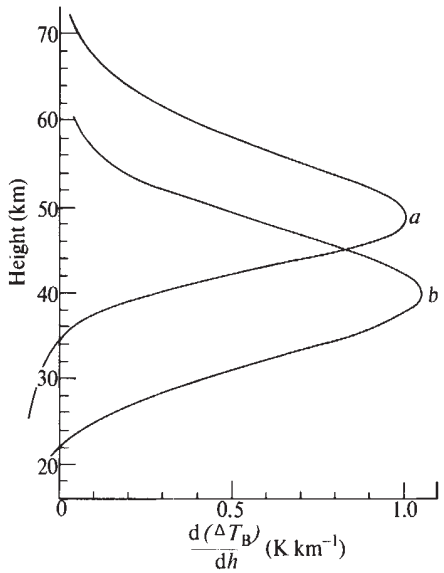


**Fig. 4** Height resolution for ground-based sensing of upper stratospheric temperatures from $O_2$ millimetre-wavelength emission. *a*, $\nu_2=\nu_0=53{,}066.9$ MHz, $\nu_1=\nu_0-2.5$ MHz; *b*, $\nu_2=\nu_0-2.5$ MHz, $\nu_1=\nu_0-20$ MHz.

The discrepancy between measured and calculated line amplitudes is significantly larger than the radiometer calibration uncertainty. The image sideband contributes a slope to the measured lines, but cannot account for the amplitude disagreement. Atmospheric temperatures must be warmer than the model used for calculations by $\sim 50$ K at altitudes of 30–60 km in order to explain the discrepancy, a highly unlikely situation for the time and location of the measurements[21], and reported anomalous $O_2$ concentrations[22] occur at altitudes too high to contribute significantly to the emission measured here. The discrepancy probably arises from the theory used for the calculations, which sums the (assumed incoherent) absorption of the individual lines. A theory which accounts for coherence in overlapping lines has been applied[23] to absorption by pure $O_2$ at a pressure of several atmospheres and gives better agreement with measurement than calculations which simply sum individual line absorption. This theory has also been used[24] to calculate $O_2$ absorption at atmospheric pressures, but quantitative comparisons with measurement have not yet been made.

Previous publications have described how millimetre-wavelength $O_2$ emission can be used to sense temperatures up through the mesosphere from satellite-based measurements[12,13,16,27] and tropospheric temperatures from ground-based measurements[25–27]. Temperatures in the stratosphere can also be sensed from ground-based measurements of the $O_2$ emission lines reported here. High altitude emission is distinguishable from low altitude emission because of the strong dependence of linewidth on altitude up to $\sim 50$ km where Zeeman splitting produces an effective linewidth that is only a weak function of altitude. Emission above $\sim 70$ km contributes negligibly to the lines because the absorption coefficient at line centre is then proportional to $O_2$ density, not to mixing ratio as when collisions dominate line broadening, and line emission decreases exponentially with altitude. Variations in absorption by the lower atmosphere can be corrected for by measurements of the base of the line. Fig. 4 shows the altitude region sensed by the ground-based measurements, where the two curves give as a function of altitude the contribution per unit altitude to the measured emission at the ground. The curve with the higher peak is for the difference in measured emission between the centre of the line and 2.5 MHz away from the centre; that with the lower peak is for the difference in measured emission between 2.5 MHz and 20 MHz from the centre of the line. The high rotational lines are sensitive functions of temperature; a 1% change in upper stratospheric temperature produces a 5% change in emission at the centre of the 27$_-$ line[2]. The instrument described here can measure upper stratospheric temperature variations with r.m.s. accuracies of $\sim 1$ K for an integration time of 1 h. Stratospheric phenomena which can be conveniently studied from the ground by this measurement technique include diurnal temperature variation[28] and sudden warmings[29].

I thank M. L. Meeks for suggesting the possibility of measuring atmospheric emission from the 27$_-$ line; A. H. Barrett, K. F. Kunzi and D. H. Staelin for helpful discussions; and J. W. Barrett, R. W. Chick, V. T. Kjartansson, D. C. Papa and R. M. Paroskie for help in constructing the radiometer. This work was supported by the National Aeronautics and Space Administration.

Received October 18; revised November 24, 1972.

1 Kahan, W., *Nature*, **195**, 30 (1962).
2 Waters, J. W., *Proc. Seventh Inter. Symp. Remote Sensing of Environment*, Univ. of Mich. (1971).
3 Carter, C. J., Mitchell, R. L., and Reber, E. E., *J. Geophys. Res.*, **73**, 3113 (1968).
4 Harries, J. E., Swann, N. R. W., Beckman, J. E., and Ade, P. A. R., *Nature*, **236**, 159 (1972).
5 Nolt, I. G., Radostitz, J. V., and Donnelly, R. J., *Nature*, **236**, 444 (1972).
6 Waters, J. W., Paroskie, R. M., Barrett, J. W., Papa, D. C., and Staelin, D. H., *Res. Lab. Elec., Q. Progress Rpt. 107*, 23 (Massachusetts Institute of Technology, 1972).
7 Weinreb, S., *Res. Lab. Elec. Tech. Rpt.*, 412 (Massachusetts Institute of Technology, 1963).
8 Wilheit, jun., T. T., thesis, Massachusetts Institute of Technology (1969).
9 Welch, W. M., and Mizushima, M., *Phys. Rev.*, A, **5**, 2692 (1972).
10 Wilheit, jun., T. T., and Barrett, A. H., *Phys. Rev.*, A, **1**, 213 (1970).
11 Van Vleck, J. H., *Phys. Rev.*, **71**, 413 (1947).
12 Lenoir, W. B., *J. Geophys. Res.*, **73**, 361 (1968).
13 Meeks, M. L., and Lilley, A. E., *J. Geophys. Res.*, **68**, 1653 (1963).
14 Zhevakin, C. A., and Naumov, A. P., *Izvest. VUZ Radiofiz.*, **9**, 433 (1966).
15 Reber, E. E., Mitchell, R. L., and Carter, C. J., *IEEE Trans. Ant. and Prop.*, AP-18, 472 (1970).
16 Croom, D. L., *Planet. Space Sci.*, **19**, 777 (1971).
17 Reber, E. E., *J. Geophys. Res.*, **77**, 3831 (1972).
18 Valley, S. L., ed., *Handbook of Geophysics and Space Environments* (McGraw-Hill, New York, 1965).
19 Waters, J. W., thesis, Massachusetts Institute of Technology (1970).
20 Gross, E. P., *Phys. Rev.*, **97**, 395 (1955).
21 Cole, A. E., *Space Research*, **11**, 813 (Akademie-Verlag, Berlin, 1971).
22 Tchen, C. M., *Space Research*, **11**, 899 (Akademie-Verlag, Berlin, 1971).
23 Gorden, R. G., *J. Chem. Phys.*, **46**, 448 (1967).
24 Mingelgrin, U., *US Dept. of Commerce Telecommunications Res. and Eng. Rep.*, 32 (1972).
25 Westwater, E. R., and Strand, O. N., *Tech. Rept. IER37–ITSA37* (US Dept. of Commerce, 1967).
26 Miner, G. F., Thornton, D. D., and Welch, W. J., *J. Geophys. Res.*, **77**, 975 (1972).
27 Staelin, D. H., *Proc. IEEE*, **57**, 427 (1969).
28 Groves, G. V., *IQSY* 5, Paper 14 (1969).
29 Barnett, J. J., Harwood, R. S., Houghton, J. T., Morgan, C. G., Rodgers, C. D., Williamson, E. J., Peckham, G., and Smith, S. D., *Nature*, **230**, 47 (1971).